# A COMPACT, LOW-PROFILE, ULTRA-WIDEBAND ANTENNA UTILIZING DUAL-MODE COUPLED RADIATORS

## Meng Li[*], Yazid Yusuf, and Nader Behdad

Department of Electrical and Computer Engineering, University of Wisconsin-Madison, 1415 Engineering Drive, Madison, WI 53706, USA

**Abstract**—In this paper, we present a low-profile, compact, ultra-wideband antenna that uses a set of closely coupled radiators. The system of two coupled radiators has two different linearly independent modes of operation with complementary frequency bands of operation. These include the differential mode and the common mode of operation. When the antenna is excited in the common mode of operation, it acts as an ultra-wideband (UWB) antenna covering a broad frequency band. When excited in the differential mode, the antenna operates as a wideband dipole in a frequency range below that of the common mode. Thus, by appropriately combining the two modes using a suitably designed feed network, the bandwidth of the antenna can be extended and its lowest frequency of operation is reduced. Mode combining is achieved with a feed network that employs a frequency-dependent phase shifter. Using this feed network, the two modes of the antenna are combined and a single-port broadband device is achieved that has a bandwidth larger than that of either the common or the differential mode individually. A prototype of the antenna is fabricated and experimentally characterized.

## 1. INTRODUCTION

Ultra-wideband (UWB)antennas have been widely used in many areas such as high data-rate wireless communication systems, sensing, radar systems, and microwave imaging [1]. In most cases, UWB antennas are required to be impedance matched and radiate efficiently over a large frequency span. In many applications (e.g., military communications at HF, VHF, and UHF frequency bands), ultra-wideband antennas

that can efficiently radiate vertically-polarized waves are required. Monopole whips are the most widely used types of antennas for such applications. However, monopoles are very high-profile structures that protrude significantly from the surfaces they are mounted on. In many applications (particularly military systems), this is highly undesirable. Additionally, in such communications applications, the antennas are usually mounted on complex platforms in the presence of other antennas and large scatterers. In such a rich scattering environment, the radiation patterns of the antenna are significantly affected by the platform it is mounted on and by the interaction between the antenna and the platform. Consequently, the radiation patterns of most conventional antennas will change significantly when they are mounted on the platform (e.g., a monopole antenna will no longer be an omni-directional radiator when mounted on a vehicle in close proximity to other scatterers). Thus, in developing UWB antennas for such applications, achieving high radiation efficiency and broadband impedance matching has a higher priority than achieving consistent radiation patterns across the entire band of operation of the antenna.

Developing compact and low-profile UWB antennas has been the subject of intense study recently. The size of a UWB antenna is mainly determined by its lowest frequency of operation. In general, the maximum linear dimension of a UWB antenna is inversely proportional to its lowest frequency of operation. Therefore, for a UWB antenna that is required to cover very low frequencies, such as VHF and UHF bands, the size of the antenna can be prohibitively large. Therefore, the demand for compact UWB antennas with high radiation efficiency and broadband impedance matching is more then ever felt. Various UWB antenna miniaturization techniques have been proposed in the past. Many of the existing UWB antennas are in the form a monopole-like radiating structures with top-loaded capacitive plates and internal matching elements (e.g., shorting pins or series inductors). One of the earliest antenna designs that falls into this category is the Goubau antenna [2], which operates over a bandwidth of about an octave (a VSWR of 3 : 1 is considered as the criteria of frequency of operation) within a cylindrical volume with the diameter of $0.18\lambda_{min}$ and the height of $0.065\lambda_{min}$ ($\lambda_{min}$ is the free-space wavelength at the lowest frequency of operation). Later on, antennas with similar performance levels were presented by Friedman [3] and Nakano et al. [4]. All of these antennas share similar topologies where top-loaded hat and shorting pins are included within the antenna structure. Despite the impressive performance of these antennas, extending their bandwidths at the lower ends of their operating bands (without increasing their occupied

volumes) has proven to be extremely difficult. More recently, a number of research groups have tackled this problem by using resistive loading or loading the antenna with lossy ferrite materials [5, 6]. While this can be used to reduce the lowest frequency of operation of the antenna and achieve good impedance matching at the lower end of the band, this comes at the expense of sacrificing the antenna gain and radiation efficiency. Thus, developing techniques that could be used to reduce the lowest frequency of operation of a UWB antenna, without increasing its occupied size and using lossy materials, is of great practical interest.

In this paper, a new technique for reducing the lowest frequency of operation of a UWB antenna is introduced that does not use lossy materials or increase the occupied volume of the structure. The proposed technique is based on using two linearly independent modes of a radiating structure that have complementary frequency bands of operation. The antenna is composed of two closely coupled radiators. When the radiators are excited in phase, they act as a coupled loop antenna, which operates over an extremely broadband frequency range extending from 600 MHz to at least 4 GHz. When the radiators are excited with a 180° phase shift, however, the antenna acts as a broadband dipole covering the frequency range of 400 MHz–600 MHz. Thus, in its differential mode of operation, the antenna operates over a frequency band that is complementary and (more importantly) below that of the common mode. Thus, by appropriately combining these two modes, the lowest frequency of operation of a coupled loop antenna can be reduced significantly, without increasing its occupied volume. The antenna shape is optimized to ensure that the two modes of operation will radiate vertically polarized waves. The two radiators are fed using a power divider/phase shifter feed network that is designed to feed the antenna in the appropriate mode of operation based on the frequency of the excitation signal. The concept of such dual-mode antenna was first proposed in [7, 8]. However, in these prior work, no attention has been paid to the radiation performances of the proposed antenna with dual-mode operation. In what follows, we will carefully examine each of these two radiation modes and describe the design of the feed network. The resulting antenna is demonstrated to have a larger overall bandwidth compared to what can be achieved by using each mode individually. Because, the two modes of the antenna have different radiation patterns and the feed network is not ideal, the radiation patterns of the proposed antenna change across its entire band of operation. However, the antenna maintains high radiation efficiency, broad impedance match, and consistent polarization across the entire band. The fact that the radiation patterns of the antenna change as a function of frequency must be taken into account in determining

whether or not this design would be suitable for a given application. It is expected that in certain applications (e.g., antennas operating in rich scattering environments or fast changing channels), this issue will not be a major source for concern. The benefit of the proposed UWB antenna with combined modes of operation is that the lowest frequency of operation of the UWB antenna can be significantly reduced without increasing its occupied volume. Such benefit offered by the combined modes of operation can be best illustrated by comparing the size of proposed antenna with that of the previous existing antenna. This comparison is conducted by evaluating the electrical height of the antennas at their respective lowest frequency of operation. The electrical height is $0.065\lambda_{\min}$ for the well-known Goubau antenna [2], $0.071\lambda_{\min}$ for the Nakano antenna [4], and $0.053\lambda_{\min}$ for the coupled sectorial loop antenna in [9]. In contrast, the proposed antenna has an electrical height of only $0.036\lambda_{\min}$ and a lateral dimension of $\sim 0.24\lambda_{\min} \times 0.24\lambda_{\min}$ at its lowest frequency of operation, and achieves a VSWR lower than $3:1$ over an extremely broad frequency band. A prototype of the proposed antenna is fabricated and measured, and its radiation performances, including radiation pattern, realized gain and efficiency, are experimentally characterized. The constraints and challenges associated with the proposed design are discussed thoroughly in the following sections.

## 2. ANTENNA DESIGN AND PRINCIPLES OF OPERATION

Figure 1 shows the three-dimensional topology of the proposed antenna. The antenna is composed of two closely-coupled loops, each of which is in the form of a bent diamond-shaped conductor mounted on top of a finite ground plane. Each loop antenna is short circuited at its end to the ground plane and fed at the center. The two loop radiators are loaded with pentagon-shaped top hats which provide capacitive loading that reduces the lowest frequency of operation of the loops. In general, these two coupled loop radiators do not have to be identical to each other. As can be seen from the side view of the antenna shown in Figure 1(b), the two loop radiators are individually fed using two coaxial connectors. Depending on the relative phase of the excitation between the two ports, the antenna can be operated in either the common mode or the differential mode. In an ideal case, such mode selection can be done by using a feed network composed of a power divider and an ideal phase shifter as shown in Figure 1(c). In an ideal operating scenario, the phase shifter provides a $180°$ phase shift over the frequency range where the antenna is expected to work in
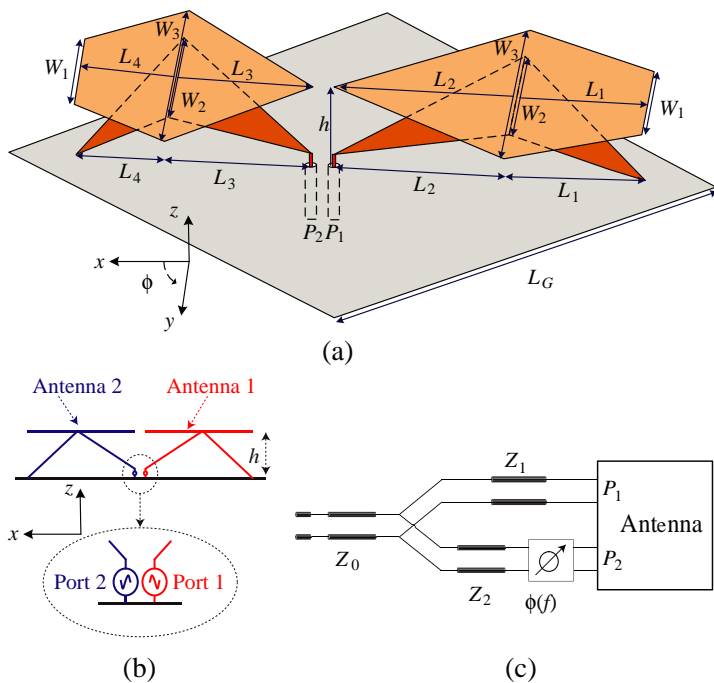
**Figure 1.** (a) Three-dimensional topology of the proposed UWB antenna. (b) Side view of the antenna demonstrating the two radiators and feeding arrangement. (c) The feeding network architecture is composed of a power divider and a phase shifter that can be used to combine the two modes of operation of the antenna.

the differential mode and a 0° phase shift in the frequency range where the antenna is supposed to work in the common mode. This way, the structure will be fed in the appropriate mode of operation based on the frequency of the excitation signal. The common mode is selected when $\phi = 0°$, and the differential mode is selected when $\phi = 180°$. In what follows, both of these two modes will be examined individually.

## 2.1. Common Mode of Operation

In the common mode, the two loop radiators are fed in phase, and the resulting structure acts as a closely-coupled loop antenna with ultra-broadband bandwidth [10]. Ultra-wideband coupled loop antennas with different shapes and topologies have been examined before. In [10], it has been demonstrated that when two loop antennas are closely coupled to each other, the variations of their mutual impedance

can cancel those of each loop's self impedance. Therefore, when the antennas are fed in phase, a relatively constant input impedance (vs. frequency) can be achieved. In this paper, the antenna topology shown in Figure 1(a) is indeed evolved by replacing the simple loop radiators in [10] with bent-diamond shaped radiators. Such evolution in the shape of the loop radiator introduces more mutual coupling between the coupled radiators, and is found to be more suitable in designing compact antennas. In [11], it was demonstrated that such coupled loop antennas can be further miniaturized by loading them with capacitive top hat plates. The top-loaded hats of the proposed antenna offer a large capacitive loading [11, 12] to reduce the lowest frequency of operation of a UWB antenna.

The current distribution of the proposed antenna in its common and differential modes of operation are examined using full-wave EM simulations in CST Microwave Studio. In the common mode, the current maxima occur near the short circuit tips and the electrical length of the antenna from the shot circuit location to the center of the antenna (where the feed is located) is approximately a quarter of a wavelength. Therefore, the majority of the radiation in this mode comes from two effective vertical electric currents that are separated from one another by a distance, which is smaller than the maximum linear dimension of the antenna. Therefore, in the common mode of operation, the antenna behaves similar to a two-element monopole antenna array with small spacing between the two elements and radiates a vertically-polarized electromagnetic wave with an omni-directional radiation pattern. In the differential mode, however, the antenna acts as a dipole antenna placed in close proximity to the ground plane. Therefore, the current flowing in one arm of the antenna will be oppositely directed to the one flowing in the other arm. Additionally, because of the bent diamond arm topology of the structure, the effective radiating currents will have both a horizontal component and a vertical component. Thus, in this mode of operation, the antenna can be thought of as two horizontally oriented electric currents placed in close proximity to a ground plane and two vertically-oriented electric currents placed vertical to the ground plane. Since the antenna height is electrically small, the radiation coming from the horizontal electric currents is suppressed but the vertically-polarized electric currents can radiate efficiently. Due to the anti-symmetric nature of the excitation, however, these vertical electric currents are oppositely directed. Therefore, the radiation pattern of the antenna (for the differential mode) is expected to exhibit a null in the azimuth plane. Figure 2 shows the input voltage standing wave ratio (VSWR) of the proposed UWB antenna with geometrical

parameters listed in Table 1. In this case, symmetric pairs of coupled loop radiators are assumed. The radiation patterns of the antenna in both modes of operation are calculated using full-wave EM simulations. Figure 3 shows the radiation patterns of the antenna in the common mode in the azimuth plane (for vertical polarization). As can be seen the antenna shows a relatively omnidirectional radiation pattern in the azimuth plane, especially at low frequencies. As frequency increases, however, the azimuthal radiation pattern starts to lose its omnidirectionality. This is mainly due to the fact that the antenna becomes electrically large at these high frequencies and the same phenomenon can be observed in almost all non body-of-revolution, compact UWB antennas [13]. Nevertheless, the simulated radiation patterns in Figure 3 demonstrate that the proposed antenna behaves as a monopole-like radiating structure in the common mode of operation. As can be seen from Figure 2, the proposed antenna exhibits an ultra-broadband range of operation in the common mode with the lowest frequency of operation at 622 MHz. This lowest frequency of operation is determined by the first resonance of each bent-diamond loop radiator that is loaded with a top hat. Although increasing the resonant length of the loop structure can decrease this first resonant frequency, it dose not necessarily mean that the lowest frequency of operation of the proposed antenna in its common mode can be easily reduced. In most cases, increasing the resonant length of the loop comes at the expense of increasing the quality factor of this resonance, which can severely deteriorate the broadband matching condition of
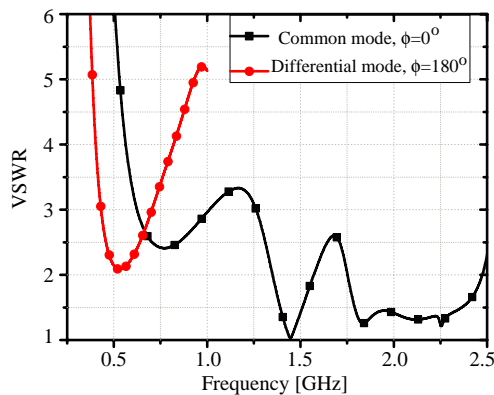


**Figure 2.** Simulated VSWR of the proposed antenna in Figure 1 with physical parameters listed in Table 1 obtained by feeding its two ports using ideal excitation coefficients.

**Table 1.** Physical parameters of the proposed antenna with symmetrical coupled loop radiators. All units are in cm.

| $L_1 = L_4$ | $L_2 = L_3$ | $L_G$ | $W_1$ | $W_2$ | $W_3$ | $h$ |
|:---:|:---:|:---:|:---:|:---:|:---:|:---:|
| 7.5 | 7 | 22 | 6.4 | 8 | 13 | 3 |

the antenna. Therefore, given a fixed antenna volume size, it becomes extremely difficult to further lower the lowest frequency of operation of the proposed antenna in its common mode of operation.

## 2.2. Differential Mode of Operation

As discussed in Section 2.1, the main challenge in the miniaturization of the proposed UWB antenna in common mode is to reduce its lowest frequency of operation while preserving the broadband impedance matching of the antenna. This can be done effectively by introducing the differential mode of operation. This differential mode can be realized by feeding the two antenna ports with a phase difference of 180° ($\phi = 180°$ in Figure 1(c)). In this mode, the two coupled loop radiators now act as one single large loop with roughly twice the circumference of each individual loops. Alternatively, the antenna in this mode can be though of as a wideband dipole which is short circuited to the ground plane at its both ends. As a result, the lowest frequency of operation in the differential mode is expected to be significantly lower than that of the common mode. This is shown in Figure 2, where the VSWRs of both common and differential modes of operation are shown for the same antenna with the physical parameters listed in Table 1. It is observed that the lowest frequency of operation of the differential mode is at 430 MHz, which is significantly lower than the lowest frequency of operation of the common mode (622 MHz). Therefore, in situations where achieving consistent radiation patterns is not of a very high priority, it can be advantageous to use the differential mode of operation to reduce the lowest frequency of operation of the antenna, since this can be done without increasing the antenna volume. A passive feed network can be designed to automatically feed the antenna in its correct mode of operation based on the input signal's frequency, as will be shown later in Section 2.3.

As we have already seen from Figure 3, in the common mode, the proposed antenna behaves like a monopole with omnidirectional radiation patterns in the azimuth plane. In the differential mode, however, the radiation patterns of the antenna will be different. As shown in Figure 4, the effective current distribution in the differential mode can be decomposed into both horizontal and vertical components.
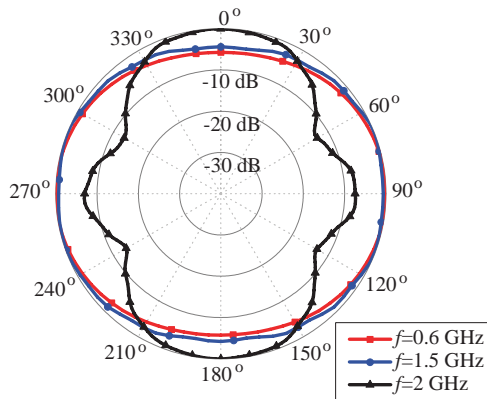
**Figure 3.** Simulated radiation patterns of the antenna shown Figure 1 with physical parameters listed in Table 1. The results show the normalized radiation patterns for the vertical polarization along the azimuth plane in the common mode of operation.

The horizontal components of the current distribution can be perceived as a horizontal dipole over perfect electric conductor (PEC) and the vertical components can be conceptually regarded as two-element monopole array with opposite excitation coefficients. The horizontal components of this effective electric current radiate in the presence of an infinite PEC ground plane and are effectively short circuited due to the small overall antenna height. Therefore, the radiation patterns of the antenna in the azimuth plane are mostly determined by the radiation patterns of the two-element monopole array that is composed of the two vertical effective radiating currents. In the azimuth plane, this array produces a vertically polarized radiated field. When perfectly symmetric coupled loop radiators are used in the proposed antenna, the corresponding excitation coefficients for these two elements will be exactly opposite with respect to each other. This, according to the canonical antenna array theory [14], will produce nulls along the axis of symmetry ($\phi = \pm 90°$ in Figure 1(a)) of the antenna. Figure 4(b) shows the radiation patterns of the antenna in the differential mode of operation obtained using full-wave EM simulations in CST Microwave Studio at 500 MHz. Clearly observed, deep nulls are created along the plane of symmetry of the antenna.

The radiation pattern of the differential mode is controlled by the excitation coefficients of the virtual two-element array depicted in Figure 4(a). While the two monopoles in this array carry currents in opposite directions, the magnitudes of their excitation coefficients can be changed by introducing an asymmetry in the topology of the
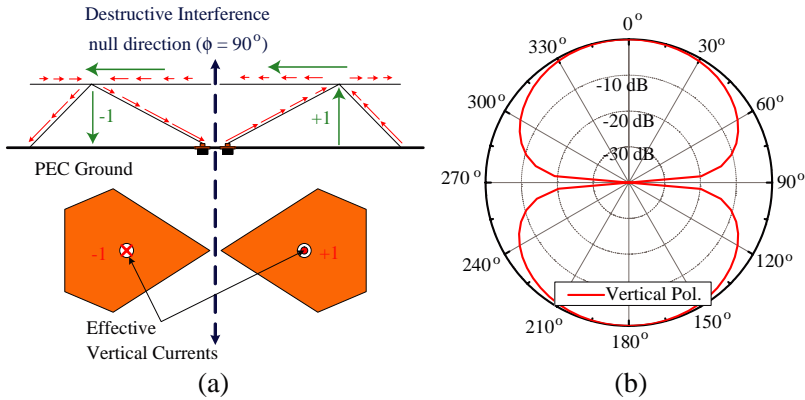
**Figure 4.** (a) The current distribution of the differential mode of a symmetric version of the proposed antenna (e.g., similar to the one having physical parameters provided in Table 1). (b) Simulated radiation patterns of the antenna with physical parameters listed in Table 1 in the azimuth plane for vertical polarization.

proposed antenna. This will reduce the depth of the null observed in the radiation patterns of the antenna in the azimuth plane. As shown in Table 2, one of the loops is made deliberately larger than the other one. The effect of such asymmetric configuration on the radiation mechanism can be best understood using the conceptual current distribution depicted in Figure 5(a). Due to the asymmetry introduced in the antenna, the excitation coefficients of the two-element array will not have the same magnitude as each other (e.g., in Figure 5(a) they are conceptually depicted as $+1$ and $-0.7$). Figure 5(b) shows the vertically polarized radiation pattern of the asymmetric antenna in the azimuth plane at 500 MHz. Clearly observed, the depth of the null is significantly reduced compared to its counterpart in Figure 4(b). The VSWRs of both common and differential modes of operation are also shown in Figure 6, where the lowest frequency of operation in differential mode (410 MHz) is observed to be roughly 1.5 times lower than that of common mode (600 MHz).

**Table 2.** Physical parameters of the proposed antenna with asymmetrical coupled loop radiators. All units are in cm.

| $L_1$ | $L_2$ | $L_3$ | $L_4$ | $L_G$ | $W_1$ | $W_2$ | $W_3$ | $h$ |
|-------|-------|-------|-------|-------|-------|-------|-------|-----|
| 5.8 | 8.1 | 6.0 | 4.3 | 22 | 6.4 | 8.0 | 13 | 3 |
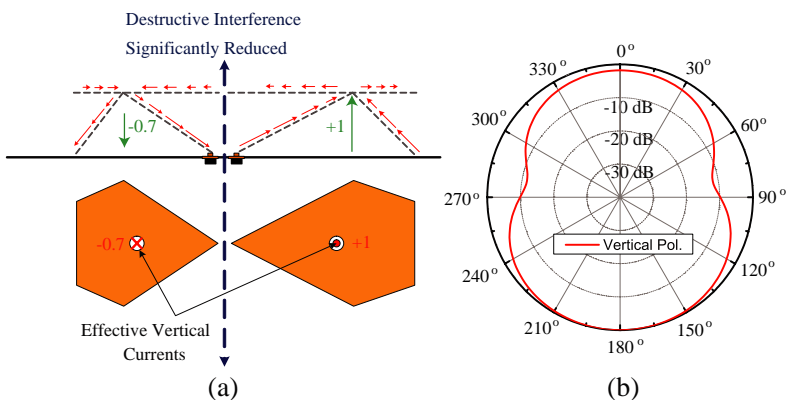
**Figure 5.** (a) The current distribution of the differential mode of an asymmetric version of the proposed antenna (e.g., similar to the one with physical parameters given in Table 2). (b) Simulated radiation patterns of the antenna with physical parameters listed Table 2 in the azimuth plane for vertical polarization.
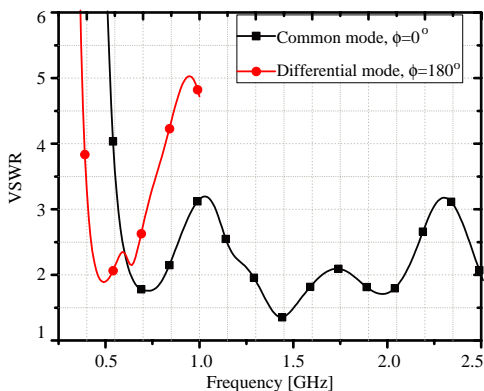


**Figure 6.** Simulated VSWR of the proposed antenna in Figure 1 with physical parameters listed in Table 2 obtained by feeding its two ports using the ideal excitation coefficients (i.e., +1 and +1 for the common mode and +1 and −1 for the differential mode).

## 2.3. Design of the Power Divider/Phase Shifter Feed Network

As mentioned previously, a key component of the proposed concept of dual-mode radiators is a feed network that can automatically feed the antenna in its correct mode of operation depending on the excitation
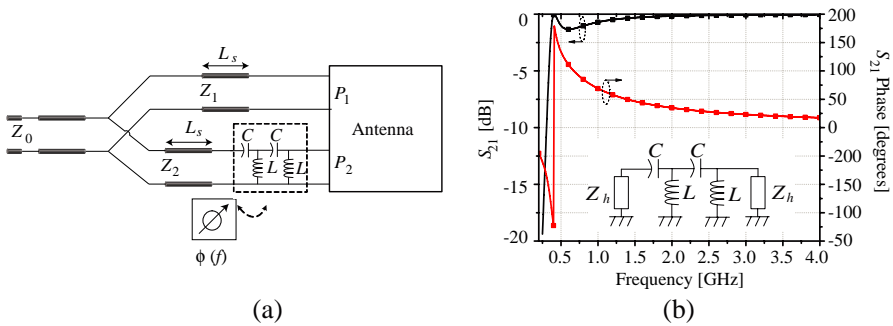
**Figure 7.** (a) The feed network used to excite the antenna in Figure 1(a). (b) The response of the lumped element frequency-dependent phase shifter in (a). Here, $Z_o = 50\,\Omega$, $Z_h = 115\,\Omega$, $L_s = 50\,\text{mm}$, $L = 23\,\text{nH}$, and $C = 3.3\,\text{pF}$.

signal's frequency. This way, a seamless transition between these two modes can be realized and from a user's perspective, the antenna works within an ultra-broadband frequency range that is larger than that the bandwidth of each mode. Such a feed network can be realized using the topology shown in Figure 7(a). The network consists of a power splitter and a frequency-dependent phase shifter. The frequency-dependent phase shifting is achieved by a lumped element high-pass network composed of capacitors and inductors. This phase shifter is designed to provide a transmission phase close to $180°$ in the frequency range of $400\,\text{MHz}$–$600\,\text{MHz}$ and a phase difference of $0°$ in the frequency range above $600\,\text{MHz}$ as shown from Figure 7(b). As can be seen from Figure 7(b), the proposed phase shifter is capable of providing a desired high transmission coefficient across all modes of operation, and an approximate $180°$ and $0°$ phase shift in differential and common mode. A sharp transition between the $180°$ and $0°$ phase shift requires a feed network with a large number of lumped elements. In this case, to simplify the design, only four lumped elements are chosen with their values listed in Figure 7(b). This frequency dependent phase shifter network will be used to combine the differential and common mode of the antenna shown in Figure 1. The microstrip lines of the feeding network are designed on a 1.6-mm-thick RT/Duroid 5880 ($\varepsilon_r = 2.2$, $\tan\delta = 0.0009$) substrate. Once the high-pass phase shifter is designed, the feed network parameters are optimized using a circuit simulator (Agilent's Advanced Design System (ADS)) in order to achieve a VSWR less than 3 over the frequency range from $360\,\text{MHz}$ to $4\,\text{GHz}$. In doing this, the $S$-parameters of the antenna obtained from full-wave EM simulations are used in the ADS simulations and optimizations.

(a)                                          (b)
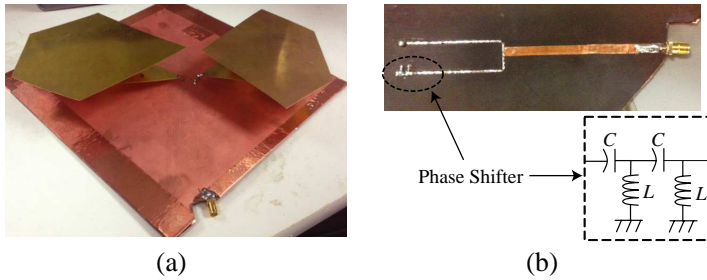
**Figure 8.** (a) The photograph of the fabricated antenna with asymmetric coupled loop radiators. The detailed dimensions of the antenna is listed in Table 2. (b) The fabricated feed network with frequency dependent phase shifter. The detailed values of lumped elements are listed in Figure 7(b).
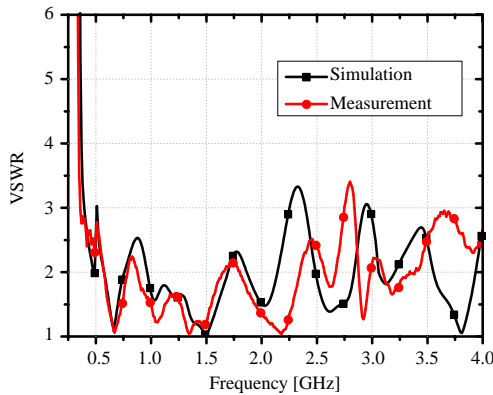


**Figure 9.** Simulated and measured VSWR of the antenna combined with the feed network.

## 3. RESULTS AND DISCUSSION

One prototype of the antenna with the detailed dimensions listed in Table 2 is fabricated and shown in Figure 8. The antenna has maximum dimensions of $20\,\text{cm} \times 20\,\text{cm} \times 3\,\text{cm}$ and has finite ground plane dimensions of $20\,\text{cm} \times 20\,\text{cm}$. The feed network is patterned on a dielectric substrate located on the bottom side of the ground plane as shown in Figure 8(b). The response of the antenna with the feed network is measured using a vector network analyzer (VNA). Figure 9 shows the comparison between the measured and simulated input VSWR of the antenna. A good agreement between

the measurement and simulation is achieved, especially at frequencies below 2 GHz. The measured lowest frequency of operation is 360 MHz, which is reasonably close to the simulated value of 390 MHz. The slight disagreement between the simulation and measurement can be attributed to the variation of the lumped element capacitor and inductor values from their nominal values. Nevertheless, the measurement results demonstrate the broadband performance of the antenna and the fact that the responses of both modes can be combined together using the proposed power divider/phase shifter feed network.

The radiation characteristics of the antenna are measured using a multi-probe near field system. Figure 10 shows the measured radiation patterns of the antenna in the frequency range of 0.4–3.0 GHz. Observe from Figure 10(a) that the antenna's radiation patterns change as frequency changes and the shape of the radiation patterns do not agree very well with the radiation patterns predicted from full-wave simulation results. There are two reasons for this. The first contributor to this is the finite size of the ground plane used in the measurement (simulation results were obtained for infinite ground plane). The second, and perhaps more important reason, is that the feed network employed in this design does not behave like an ideal feed network. In particular, the feed network performs perfectly well when the two outputs of the network (shown in Figure 7(a)) are connected to fixed impedances. However, the impedance of the antenna is not fixed and changes with frequency. This changes the response of the feed network from the ideal response (e.g., the one shown in Figure 7). This results in variation of the radiation patterns of the antenna versus frequency.
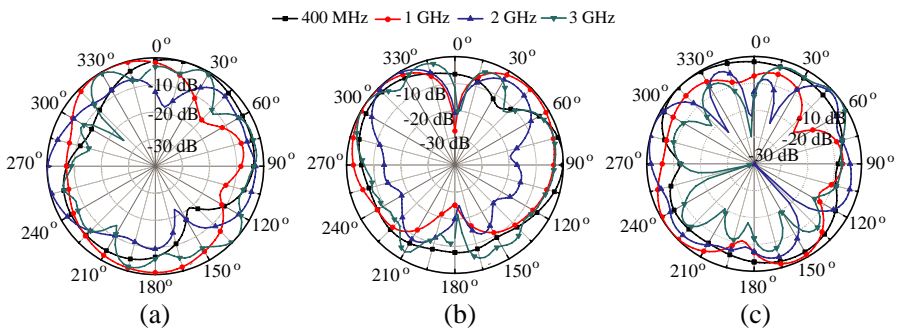


**Figure 10.** Measured normalized radiation patterns (vertically polarized) of the antenna in the azimuth $x$-$y$ and two elevation planes $x$-$z$ and $y$-$z$. (a) Azimuth ($x$-$y$) plane. (b) Elevation plane ($x$-$z$). (c) Elevation plane ($y$-$z$).

The radiation patterns in two elevation planes ($x$-$z$ and $y$-$z$ planes) are also shown in Figure 10(b) and Figure 10(c). As can be seen, a significant amount of radiation exists in the lower hemisphere (below the ground plane). This is due to the fact that the antenna has finite ground plane size of $20\,\mathrm{cm} \times 20\,\mathrm{cm}$, which is the same as the antenna's maximum lateral dimensions. Similar to any other monopole type radiator, as the ground plane size increases, the radiation levels below the ground plane decreases. However, due to the limitations of the sizes of antennas that we could measure using the available setup, the radiation patterns of this antenna with a larger ground plane were not measured.

The gain and radiation efficiency of the antenna are also measured using the same near-field system. The measured realized gain of the antenna, which includes the impedance mismatch effects, is shown in Figure 11. Notice that the antenna gain can be increased if the antenna is mounted on a large platform or if the ground plane size is increased. The radiation efficiency of the antenna is also measured using the same multi-probe near field system and the results are presented in Figure 11 as well. Over most of the operating band, the radiation efficiency remains above 75%.
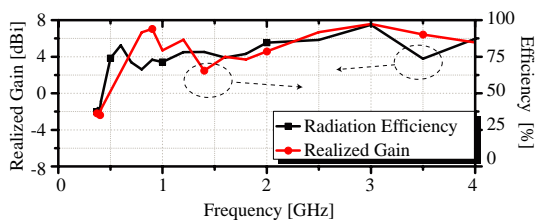


**Figure 11.** Measured realized gain and the radiation efficiency of the antenna. The gain values reported take into account the effect of the impedance mismatch.

## 4. CONCLUSIONS

In this paper, the concept of closely-coupled, dual-mode radiators is utilized to design a compact, low-profile, ultra-wideband antenna. Two distinct modes of operation with complementary frequency bands of operation are exploited in the design. The proposed antenna behaves as a top-hat loaded, coupled loop antenna with ultra-broadband frequency response in its common mode of operation and it acts as a wideband dipole with bent-diamond shaped arms in the differential mode of operation. The frequency of operation of the differential

mode is complementary to and below that of the common mode. These two modes are combined together using a feed network that uses a frequency-dependent lumped element phase shifter. The resulting antenna has a larger overall bandwidth compared to what can be obtained using each mode individually. More importantly, the combining of the two radiating modes allows for reducing the lowest frequency of operation of an ultra-wideband antenna while maintaining its occupied volume. The primary limitation of the proposed approach, i.e., the variation of radiation patterns, was also discussed. In particular, the inconsistencies of the antenna's radiation pattern as a function of frequency is the main price that is paid for using this approach. This might be overcome to some extent by using a rotationally symmetric version of this antenna and exploiting techniques such as quadrature feeding. In its current form, we envision that this antenna will be most suitable for applications where having a high radiation efficiency and broadband operation is more important than having consistent radiation patterns or a specific shape of radiation patterns.

## ACKNOWLEDGMENT

## REFERENCES

1. Schantz, H., *The Art and Science of Ultrawideband Antennas*, Artech House, Norwood, MA, 2005.

2. Goubau, G., N. N. Puri, and F. Schwering, "Diakoptic theory for multielement antennas," *IEEE Trans. Antennas and Propag.*, Vol. 30, No. 1, 15–26, 1982.

3. Friedman, C. H., "Wide-band matching of a small disk-loaded monopole," *IEEE Trans. Antennas and Propag.*, Vol. 33, No. 12, 1142–1148, 1985.

4. Nakano, H., H. IWaoka, K. Morishita, and J. Yamauchi, "A wideband low-profile antenna composed of a conducting body of revolution and a shorted parasitic ring," *IEEE Trans. Antennas and Propag.*, Vol. 56, No. 4, 1187–1192, 2008.

5. Moon, H., G.-Y. Lee, C.-C. Chen, and J. L. Volakis, "An extremely lowprofile ferrite-loaded wideband VHF antenna design," *IEEE Antennas Wirel. Propag. Lett.*, Vol. 11, 322–325, 2012.

6.  Palud, S., F. Colombel, M. Himdi, and C. L. Meins, "Wideband omnidirectional and compact antenna for VHF/UHF band," *IEEE Antennas Wirel. Propag. Lett.*, Vol. 10, 3–6, 2011.

7.  Yusuf, Y. and N. Behdad, "Compact, low-profile UWB antennas exploiting the concept of closely-coupled dual-mode radiators," *IEEE Antennas and Propagation Society International Symposium (APSURSI)*, 1–2, Jul. 8–14, 2012.

8.  Yusuf, Y. and N. Behdad, "Miniaturization of a class of ultra-wideband antennas using dual-mode radiating structures," *2012 IEEE International Conference on Wireless Information Technology and Systems (ICWITS)*, 1–4, Nov. 11–16, 2012.

9.  Elsherbini, A. and K. Sarabandi, "Very low-profile top-loaded UWB coupled sectorial loops antenna," *IEEE Antennas Wirel. Propag. Lett.*, Vol. 10, 800–803, 2011.

10. Behdad, N. and K. Sarabandi, "A compact antenna for ultrawide-band applications," *IEEE Trans. Antennas and Propag.*, Vol. 53, 2185–2192, 2005.

11. Behdad, N., M. Al-Joumayly, and M. Salehi, "Ultra-wideband low profile antenna," US Patent No. 8,228,251, 2012.

12. Seeley, E. W., "An experimental study of the disk loaded folded monopole," *IRE Trans. Antennas Propag.*, Vol. 4, No. 1, 27–28, Jan. 1956.

13. Baum, C. E., A. P. Stone, and J. S. Tyo, *Ultra-wideband, Short-pulse Electromagnetics 8,* Springer, New York, 2007.

14. Balanis, C. A., *Antenna Theory: Analysis and Design*, 3rd edition, Wiley-Interscience, 2005.